PHENIX highlights: Recent results from PHENIX

Maya Shimomura[1,2,] for the PHENIX Collaboration *

[1]Department of Mathematical and Physical Sciences, Nara Women's University
[2]RIKEN Nishina Center

Abstract. The Relativistic Heavy Ion Collider (RHIC) PHENIX experiment has provided new insights into the behavior of quark-gluon plasma (QGP) under extreme conditions. While PHENIX concluded data collection in 2016, the collaboration remains actively engaged in analyzing the rich dataset yielding the following three important results recently. (1) Heavy flavor (HF) with charm and bottom quark separation indicates a clear mass dependence observed in central collisions. Additionally, forward rapidity J/ψ and v_2 measurements show a result consistent with zero, in contrast to LHC findings. (2) Precise direct photon yields obtained via large statistical datasets, spanning a wide range of transverse momentum (p_{T}) and centrality bins have the scaling behavior across various large systems, and non-prompt direct photon results reveal temperature (T_{eff}) dependence on p_{T}. (3) Charged hadron production was examined in collision systems of varying sizes, revealing that R_{AA} is primarily dependent on the overlap volume (N_{part}). Moreover, R_{dAu} obtained by experimental N_{coll} suggests the clear yield suppression in central collisions.

1 Introduction

Quark-gluon plasma (QGP) is a state of matter in which quarks and gluons are no longer confined within hadrons. The study of this extreme state of matter has been one of the major topics in high-energy nuclear physics for several decades. The Relativistic Heavy Ion Collider (RHIC) at Brookhaven National Laboratory (BNL) in the United States has played a central role in deepening our understanding of this phase. The RHIC PHENIX (Pioneering High Energy Nuclear Interaction Experiment) experiment has obtained accumulated extensive data for nine collision species and nine collision energies, providing crucial experimental insights into the properties of QGP under temperatures and energy densities similar to those found in the early universe.

Since its first operation in 2000, PHENIX has produced numerous significant experimental results. For instance, the discovery of strong elliptic flow (v_2) in non-central collisions provided important evidence for the collective motion of the QGP, suggesting that its viscosity is extremely low, consistent with nearly perfect fluid behavior. Furthermore, the observation of yield suppression at high transverse momentum, commonly referred to as jet quenching, revealed that QGP strongly interacts with high transverse momentum partons produced only in the initial collision stages, leading to significant energy loss.

Although data collection concluded in 2016, the PHENIX collaboration remains highly active, continuing to produce new results based on the extensive data set. Recent studies

*e-mail: maya@cc.nara-wu.ac.jp

have reported new findings on the interactions of heavy-flavor quarks, the production of direct photons, and charged hadron production in various collision systems. These analyses represent important steps toward a deeper understanding of QGP properties and dynamics, contributing not only to mapping the QCD phase diagram but also to research on the boundary conditions for QGP production and comparisons with results from the LHC. This paper focuses on reporting these recent findings.

2 Results from heavy flavor production

The first topic is the heavy flavor at mid and forward rapidity measured by PHENIX. The details of this study are discussed here [1] also. Heavy-flavor quarks (HQ), such as charm (c) and bottom (b), provide a valuable probe for studying the properties of the quark-gluon plasma (QGP) due to their large mass. At RHIC energies, heavy-flavor quarks are primarily produced during the initial hard scattering phase of the collision. Their production can be accurately calculated using perturbative QCD, as their large mass restricts their creation to the early stages of the collision. Once produced, heavy-flavor quarks do not disappear but pass through the QGP, experiencing energy loss through interactions with the QGP medium. This interaction, along with their contribution to the collective motion of the QGP (flow), modifies heavy-flavor production a sensitive indicator of QGP properties.

In PHENIX, the charm and bottom quarks were successfully separated and measured. The transverse momentum (p_{T}) spectra of charm hadrons and bottom hadrons were obtained for several centrality bins [2]. These results allow for a detailed study of the mass dependence of heavy-flavor interactions with the QGP.

We also calculated the nuclear modification factor (R_{AA}) for the various centralities. The left panel in Figure 1 shows the results for central collisions (0-10%), while the right panel presents the results for peripheral collisions (40-60%) as a function of the electron transverse momentum (p_{T}). In the 0-10% centrality range, a clear suppression of both bottom and charm quarks is observed, with a distinct difference in the degree of suppression at mid p_{T}. However, in the 40-60% peripheral collisions, the suppression of both bottom and charm quarks is much smaller and their suppression patterns are similar. This indicates a clear centrality dependence as well as mass ordering in the suppression.

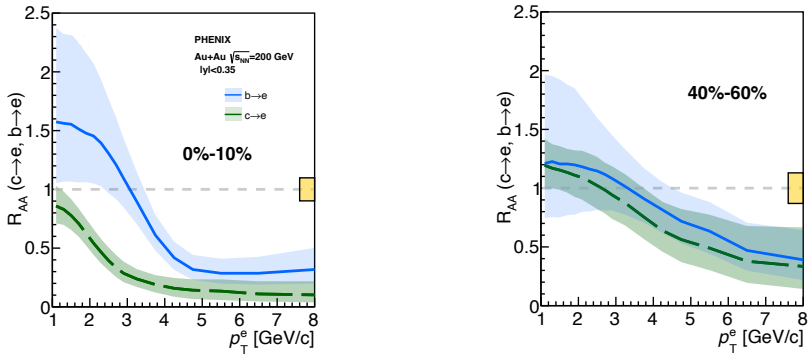

Figure 1. Central (Left) and peripheral (Right) R_{AA} for b and c decayed electron separately in Au + Au. [2]

In addition to these results, we measured the elliptic flow (v_2) of heavy-flavor muons at forward rapidity and compared it to what is obtained at mid-rapidity. The v_2 of heavy-flavor

quarks is positive at both forward and mid-rapidity, and the results are mostly consistent. In contrast, the v_2 of charged hadrons, which are predominantly composed of light quarks, is larger than that of heavy-flavor quarks. At mid-rapidity, we further separated the v_2 measurements for the charm and bottom quarks. The left panel in Figure 2 shows the v_2 for charm quarks, while the middle panel shows the v_2 for bottom quarks, compared with the v_2 of charged hadrons. As expected from mass order, the v_2 of charm quarks is larger than that of bottom quarks, while charged hadrons exhibit the largest v_2.

We also measured the v_2 of J/ψ at forward rapidity and found that it is consistent with zero, as shown in the right panel in Figure 2. The red points represent the PHENIX results, while the blue points correspond to the LHC-ALICE data, which are not consistent with zero. The R_{AA} for central collisions at RHIC and LHC energies have also significant differences [6]. These results are consistent with the regeneration scenario of charm and anti-charm quarks at LHC energies.

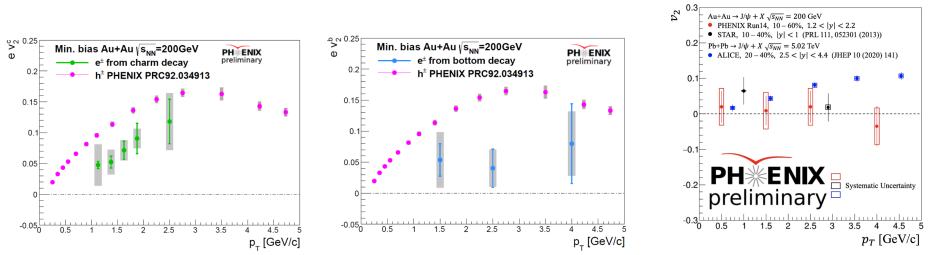

Figure 2. v_2 for b (left) and c (right) decayed electron at mid-rapidity and for J/ψ at forward in Au + Au.

3 The results of direct photon measurements

PHENIX measures direct photon production with large statistics. Figure 3 shows direct photon R_γ vs. p_T, with different centrality intervals for each panel [3]. The different panel shows different centrality [3]. External conversion method and large statistics give a precise measurement for wider p_T ranges for all measured centrality bins. Red points are new results that are consistent with previous measurements shown here but have much less uncertainty. $dN_{\text{direct photon}}/d\eta$ as a function of the $dN_{ch}/d\eta$ at mid-rapidity. The scaling of the yields holds for various large systems and is different from the p+p scaled by N_{coll} as expected.

A significant enhancement is observed at low p_T when comparing scaled p+p spectra to the central Au+Au one. Same comparisons but different system sizes are also obtained such as Au+Au peripheral, p+Au central, p+Au minimum-bias, and p+p. It seems that this enhancement is related to QGP size [3].

Non-prompt photons were extracted to gain more insight. The left panel in Figure 4 is the ratio of the spectra data to exponential fit where the effective temperature is fixed to a certain value. The ratio has clear p_T dependence but not centrality. Then we applied two different p_T ranges for fitting where the effective temperature is a free parameter and obtained the right figure in Figure 4. The result shows the effective temperature is also p_T dependent, but not dependent on the multiplicity. More details are discussed at [3].

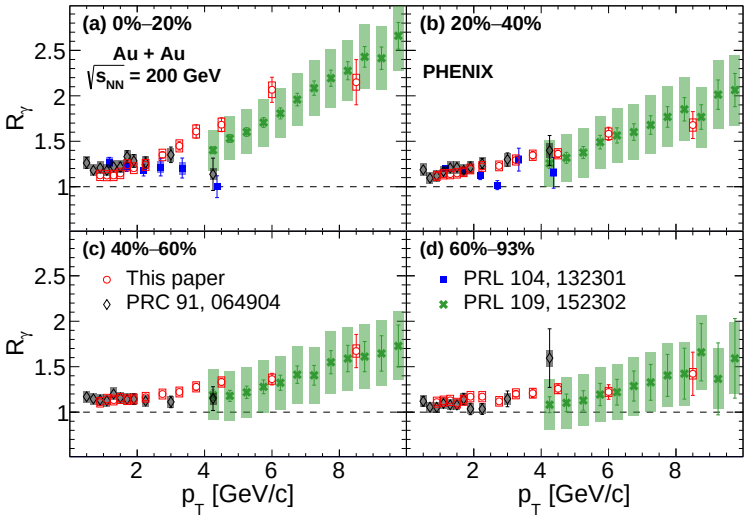

Figure 3. R_γ for direct photon measurement vs. p_T and increasing centrality intervals (panels (a) to (d)).

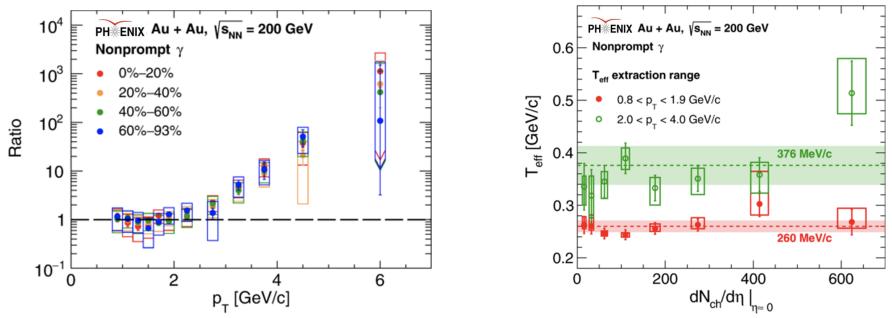

Figure 4. The left panel is the ratio of the spectra data to exponential fit where the effective temperature is fixed to a certain value in Au + Au while the right panel shows the effective temperature vs. $dN/d\eta$ for two indicated p_T ranges [3].

4 Results from PID charged hadron production

Systematics studies of hadron production are performed with PHENIX [4]. Similarly to inclusive charged hadrons, R_{AA} for PID hadrons in both large and small systems depend on collision overlap size (N_{part}) but not collision systems. Figure 5 shows R_{dA} for ϕ, π, K and proton for small colliding systems ($p + Al$, $^3He + Au$) as a function of p_T. It shows that ϕ meson has a similar trend to other mesons such as π and K and these are consistent with unity at high p_T.

For d+Au we developed the new method to calculate N_{coll} with direct photon measurement [7]. The left figures in Figure 6 are p_T spectra. π^0, direct photons spectra and their ratio as a function of p_T are shown in the top, middle, and bottom panels respectively. Since the direct photon at high p_T is not suppressed, N_{coll} can be redefined by the direct photon ratio of

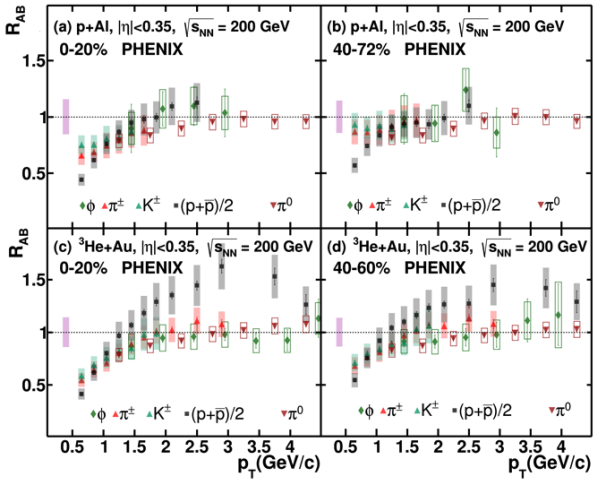

Figure 5. PID $R_{\rm AB}$ of ϕ, π, K and $p + \overline{p}$ for small colliding systems as a function of $p_{\rm T}$. ϕ meson has a similar trend to other mesons such as π and K.

d+Au to p+p experimentally as following this equation.

$$N_{\rm coll}^{\rm EXP}(p_{\rm T}) = \frac{Y_{d{\rm Au}}^{\gamma^{\rm dir}}(p_{\rm T})}{Y_{pp}^{\gamma^{\rm dir}}(p_{\rm T})}. \tag{1}$$

The right figures in Figure 6 are the calculated experimental $N_{\rm coll}$ compared with Glauber MC $N_{\rm coll}$. You can see for 0-100% centrality, $N_{\rm coll}$ Glauber and $N_{\rm coll}$ experiment agree well. However, if we divide into certain centrality bins, these are different. To avoid the $N_{\rm coll}$ Glauber bias at small system, we use this experimental $N_{\rm coll}$ to re-calculate $R_{\rm AA}$.

Figure 7 shows the re-defined $R_{\rm dA}$ with experimental $N_{\rm coll}$ for different centrality as a function of $p_{\rm T}$, and the average of these $R_{\rm dA}$ is plotted at right figure as a function of the $N_{\rm coll}$. The clear suppression can be seen at central in d+Au while it's consistent with unity in peripheral d+Au. Therefore, we could conclude there is a suppression at the central [7].

5 Summary

Recent PHENIX results are summarized. c/b separated heavy flavor $R_{\rm AA}$ and v_2 are successfully measured at various centrality bins and clear mass dependence can be seen at central. Measurement of the forward J/ψ v_2 is also performed and it's consistent with zero, and unlike LHC results, it is consistent with the regeneration scenario of charm and anti-charm at LHC energy. External conversion method and large statistics give precise measurement for wide $p_{\rm T}$ ranges and all centrality bins, and the scaling of yields holds for various large systems. Non-prompt direct photons are extracted and show the $T_{\rm eff}$ has the dependence of the $p_{\rm T}$. PHENIX measured charged hadron production at small to large collision systems and found mostly $R_{\rm AA}$ only depends on overlap volume ($N_{\rm part}$). Experimental $N_{\rm coll}$ gives non-GL biased $R_{\rm dAu}$, and indicates the clear yield suppression for central collisions.

References

[1] Luis Bichon, these proceedings.

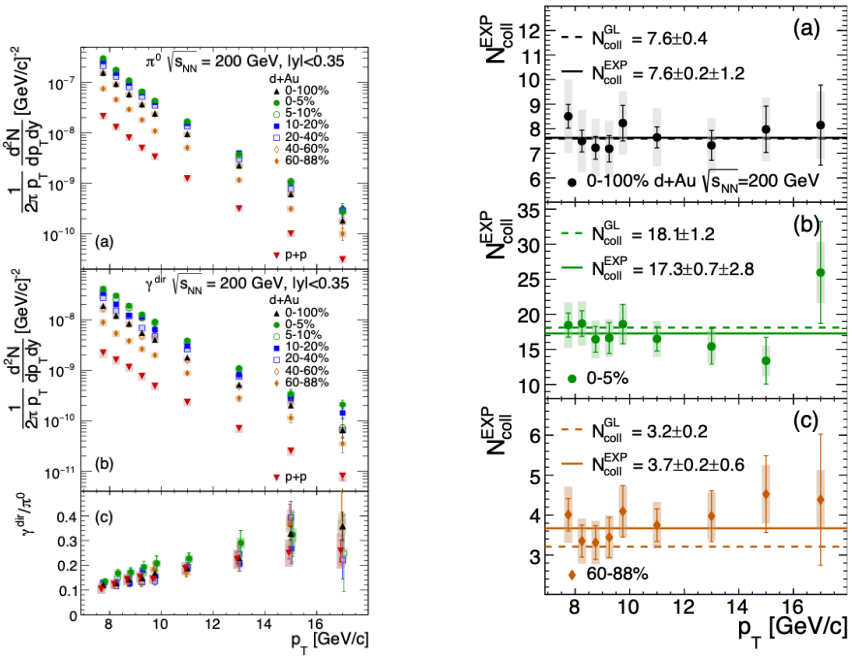

Figure 6. Left panels are p_{T} spectra for π^0 (top), direct photons (middle), and the ratio (bottom). The right panels show the calculated experimental N_{coll} compared with Glauber MC N_{coll} [7].

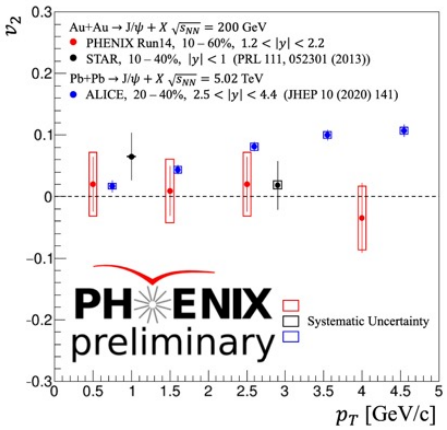

Figure 7. Nuclear modification factor for π^0 with the experimental N_{coll}.

[2] PHENIX Collaboration, Phys Rev C **109**, 044907 (2024).
[3] PHENIX Collaboration, Phys Rev C **109**, 044912 (2024).
[4] PHENIX Collaboration, Phys Rev C **109**, 054910 (2024).
[5] PHENIX Collaboration, Phys Rev C **107**, 014907 (2023).
[6] PHENIX Collaboration, Phys Rev C **84**, 054912 (2011).
[7] PHENIX Collaboration, https://doi.org/10.48550/arXiv.2303.12899